Microwave Integrated Tunnel-Diode Amplifiers for Broad-Band High-Performance Receivers

HERMAN C. OKEAN, SENIOR MEMBER, IEEE, AND PAUL J. MEIER, SENIOR MEMBER, IEEE

Abstract—**The design and development of microwave integrated-circuit (MIC) tunnel-diode amplifiers for use in integrated broad-band high-performance receivers is described. In particular, this paper describes the design, construction, and performance of thin-film microstrip tunnel-diode amplifiers operating in the 8- to 12- and 6- to 8-GHz bands, respectively, with noise figures in the 5- to 7-dB range.**

I. Introduction

THIS PAPER describes the design and development of microwave integrated-circuit (MIC) tunnel-diode amplifiers (TDAs) for use in integrated broad-band high-performance receiving systems. It describes the requirements on these amplifiers for use in such receivers, the impact of MIC technology on their construction and performance, and presents specific embodiments of thin-film microstrip 8- to 12- and 6- to 8-GHz tunnel-diode amplifiers.

II. General Aspects of the MIC Tunnel-Diode Amplifier Design

Tunnel-diode RF preamplifiers at frequencies from *C* to *K* band are finding increasing application in broad-band high-performance receiving systems, primarily to improve the sensitivity of the microwave receiver front ends used therein, both in wide-open RF-to-video and complex multiconversion superheterodyne receiver channel configurations. (Transistor amplifiers fulfill this role at frequencies below *C* band.) The desirable attributes of tunnel-diode amplifiers for this application include:

1) wide instantaneous bandwidth: half octave or greater;
2) reasonable power gain ($\geq$15 dB) to mask out noise contributions of following components in given receiver channels;
3) low noise figure ($\lesssim$6 dB);
4) reasonable instantaneous dynamic range ($\gtrsim$40 dB) between extremes of tangential sensitivity and onset of gain compression;[1]
5) compatibility with external mechanisms for dynamic range enhancement [1], input desensitization, and input limiting and/or blanking for receiver protection;
6) potential for high degree of gain and phase tracking between identical amplifiers in multiple channel systems.

MIC technology imparts the following advantages with respect to the construction of the TDAs under consideration:

1) enhancement of bandwidth capability by use of low-parasitic semiconductor active devices;
2) enhancement of bandwidth, stability against spurious oscillations, and unit-to-unit reproducibility (tracking) by elimination of all internal connectors and superfluous lengths of transmission lines;
3) ability to accommodate lower impedance and/or multiple chip devices in a closely integrated geometry, and thereby enhance large-signal capability;
4) general small size, lightweight, low cost, mass reproducibility, and increased reliability.

The individual amplifiers and associated components considered were each fabricated in microstrip transmission line on 25-mil thick alumina substrates. The vacuum-deposited thin-film metallization, comprising the conductor pattern and ground plane on the upper and lower substrate surfaces, consists of a composite chromium–copper film with the copper conductor layer thickness being about 0.1 mil and the chromium underlayer providing the necessary adhesion, as well as a medium for realization of film resistors. The conductor pattern is photoetched on the upper surface of the substrate, and the entire metallization is then gold flashed.

Accordingly, the tunnel-diode amplifiers described here are single- and dual-stage 8- to 12- and 6- to 8-GHz configurations in thin-film microstrip which typically exhibit 7- to 9-dB gain per stage and noise-figure ranges as low as 5.0 to 6.0 dB over bandwidths up to a half octave. This represents a considerable advance in performance with respect to previously reported MIC TDAs [3]–[6]. Fig. 1 shows a block diagram of a two-stage TDA including an output isolator per stage. These dual-stage TDAs are also the first MIC implementations of a multistage cascade using Ge and GaAs tunnel diodes in the input and output stages, respectively, to simultaneously optimize noise performance and dynamic range [1], [7].

Manuscript received February 24, 1971; revised June 4, 1971. This work was supported by the Air Force Avionics Laboratory (Advanced Electronics Devices Branch), Wright Patterson Air Force Base, Dayton, Ohio, under Contract F-33615-69-C-1859.

H. C. Okean was with AIL, Division of Cutler-Hammer, Melville, N. Y. He is now with LNR Communications, Inc., Farmingdale, N. Y. 11735.

P. J. Meier is with AIL, Division of Cutler-Hammer, Melville, N. Y. 11746.

[1] Several techniques may be readily used to augment the normally modest saturation-level capabilities of TDAs in a cascaded RF amplifier configuration. These include the use of low impedance and/or a multiple array of GaAs tunnel diodes in a TDA output stage and the use of a selectable sensitivity-gain control mechanism, either internal or external to the TDA cascade [1].

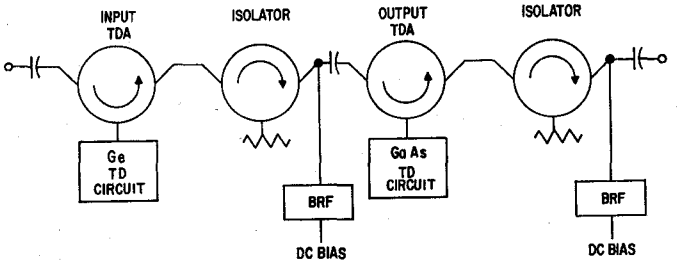

Fig. 1. Block diagram of two-stage TDA.

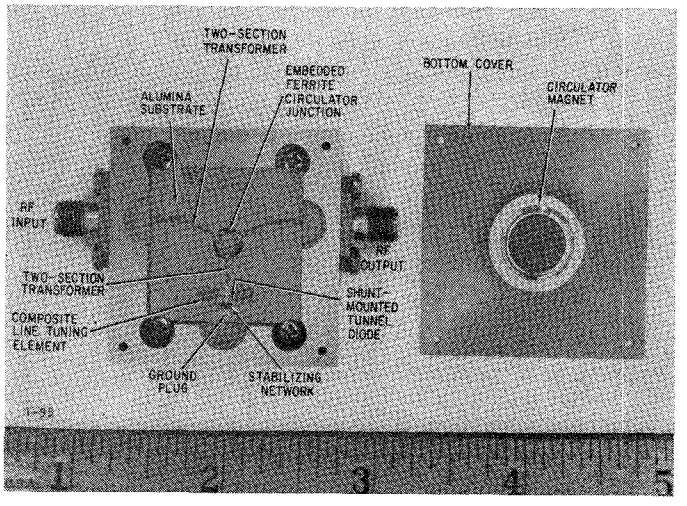

Fig. 2. Single-stage 8- to 12-GHz thin-film microstrip TDA.

The following sections describe the theoretical design, MIC implementation, and the measured performance of the individual TDA stages and the various elements used therein. In addition, the integration and packaging details and the measured performance of the dual-stage configurations will be discussed.

III. 8- to 12-GHz MIC Tunnel-Diode Amplifiers

A. Development of Individual TDA Components

Fig. 2 shows the physical embodiment of a single thin-film microstrip circulator-coupled 8- to 12-GHz TDA stage. The TDA stage is comprised of the following components which are formed on a 1-in^2 alumina substrate.

1) An encapsulated tunnel diode in a micropill package is shunt mounted through a hole in the substrate between the conductor pattern and the ground plane. Because of the high degree of compatibility of this encapsulation (50-mil dimaeter and 20-mil "active" height, and utilizing an alumina support ring within the package) with the 25-mil height alumina microstrip environment, the parasitics associated with this shunt-mounting configuration are not much in excess of those associated with series-mounted beam-lead tunnel diodes [5], [6]. This is particularly true in the normal shunt-tuned mode of TDA operation in which a dc or RF ground return (which adds to the diode series inductance by at least 50 pH) is required. Suitable commercially available tunnel diodes in this encapsulation exist in both the conventional "ball-alloy" construction [8] and in the more advanced planar "solid structure" construction [9]. The former provides superior electrical characteristics at this time; hence, both Ge and GaAs tunnel diodes of this construction were used in the TDAs described here. However, the solid-structure diodes are ultimately preferred due to their superior structural properties and potential reliability.

2) An embedded 200-mil YIG disk, metallized as above, forms the three-port circulator junction. The dc bias field for the disk is provided by an appropriately mounted platinum–cobalt magnet.

3) A pair of parallel composite open stubs, provides a parallel inductive tuning element for the tunnel diode without shorting the externally applied dc bias.[2]

4) A parallel-connected lumped-band rejection-type stabilizing network prevents out-of-band oscillations, yet appear completely reactive in the amplifier pass-band.

5) Dual quarter-wave transformers at each port of the circulator junction provide a wide-band match to the 50-Ω microstrip/3-mm coaxial input and output transducers, and provide a specified three-pole reflection gain response at the amplifier port at a particular midband gain level.

Prior to realization of the single-stage TDA (see Fig. 2), some of the individual 8- to 12-GHz thin-film microstrip circuit elements comprising it required individual development. These included the three-port circulator (and related output isolator), the stabilizing network, and the active TDA termination comprising the tuned and stablized tunnel diode.

An 8- to 12-GHz thin-film microstrip three-port circulator forms the coupling mechanism for each TDA stage, and also forms the basis for the interstage isolators in the dual-stage amplifier configuration. It is a distributed wye-junction circulator whose junction is formed by an appropriately metallized (as described in the preceding section) polycrystalline YIG disk[3] embedded in a mating hole in the alumina substrate. The metallized conductor pattern and ground plane on the top and bottom, respectively, of the YIG disk are interconnected with their counterparts on the alumina substrate via welded ribbon leads. In addition to the embedded ferrite wye-junction, each circulator typically includes impedance transformers and/or reactive match-

[2] DC bias is provided via an RF-isolated bias-feed network at one port of an output isolator which follows the TDA stage in its normal deployment.

[3] Xtalonics X-1780 (1780-G saturation magnetization). This composite configuration was chosen rather than an all-ferrite structure due to the increased losses and less well-defined junction interface associated with the latter [6].

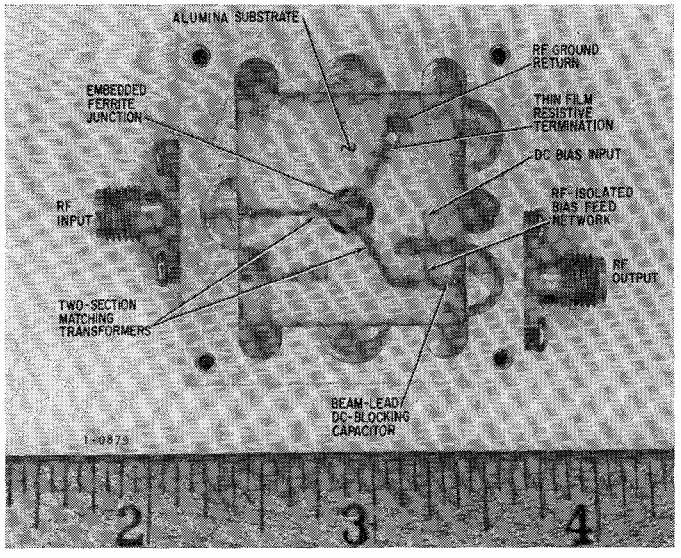

Fig. 3. 8- to 12-GHz thin-film microstrip isolator.

ing elements which interconnect the three junction ports to their respective external terminations. The magnetic bias field for the circulator junction is provided by a platinum–cobalt permanent magnet mounted in the housing directly below the substrate ground plane at the junction, as will be shown subsequently.

The measured 8- to 12-GHz admittance locus of the circulator junction, embedded in a thin-film microstrip 50-Ω three-port circuit and obtained at an optimum combination of ferrite diameter and bias field, yields a series-LC/parallel-RLC junction equivalent circuit at a 35-Ω junction impedance level with low-selectivity parallel and series bandpass reactive components centered at 10 GHz. Broad-band matching of the measured junction impedance locus to the external 50-Ω impedance level over the 8- to 12-GHz band is accomplished by including an identical two-section cascaded line impedance transformer at each junction port.

Measurements on a breadboard model of a symmetrical thin-film microstrip three-port circulator, based on this design and fabricated on a 1-in^2 alumina substrate, yielded an average of 18- to 27-dB isolation and 0.6- to 1.2-dB insertion loss per pass over the 8- to 12-GHz frequency range between each pair of adjacent ports.

This 8- to 12-GHz thin-film microstrip circulator design was used in both the amplifier circulator and each interstage isolator. The latter, formed on a 1-in^2 alumina substrate, is shown in Fig. 3. In the former, matching on the amplifier port was for a specified reflection gain response; whereas, in the latter, the isolated port was terminated internally in a thin-film 50-Ω resistor which is RF grounded by a low-impedance quarter-wave open-circuited resonator. This termination, measured individually, exhibited a ratio of less than 1.15:1 VSWR over the 8- to 12-GHz range. Also included on the isolator output arm (Fig. 3) is a three-pole RF-isolated dc bias feed network (RF isolation > 26 dB and VSWR < 1.2:1 over 8 to 12 GHz) which is used to provide dc bias voltage to the TDA stage preceding it, and a beam-lead dc blocking capacitor directly preceding the output microstrip-to-coaxial transition. The average measured performance of a group of these isolators included 16- to 25-dB isolation per pass (overcoupled response), 0.5- to 1.5-dB insertion loss per pass, and 1.15 to 1.35:1 VSWR over the 8- to 12-GHz range.

The tunnel-diode stabilizing network (Fig. 2) consists of the series combination of a thin-film resistor and a parallel resonant (at 10 GHz) LC circuit connected directly in parallel with the tunnel diode. The latter is formed by the parallel combination of a pair of electrically short open-circuited stubs and a short-circuited stub, which is grounded through the substrate by a low-inductance metallic plug. This network terminates the tunnel diode in a low-resistance R_{st} outside the amplifier passband, thereby preventing out-of-band oscillations, and appears as a completely reactive parallel LC resonator within it.

Individual measurements on this stabilizing network in the optimum thin-film microstrip geometry over the 0- to 18-GHz range yielded a monotonic circular admittance locus, which was extremely close to its theoretical counterpart, thus exhibiting an out-of-band resistance $R_{st} \approx 35\ \Omega$, and a negligible residual passband normalized shunt conductance ($G_p R_{st} \lesssim 0.14$) over the nominal 8- to 12-GHz amplifier passband.

The tuned and stabilized tunnel diode comprising the active TDA termination consists of the parallel combination of a shunt-mounted encapsulated micropill tunnel diode,[4] the previously mentioned stabilizing network, and an identical pair of inductive tuning branches. Each tuning branch consists of a short section of high-impedance (inductive) transmission line in cascade with a low-impedance quarter-wave open-circuited stub, of which the former contributes to the resonating of the capacitive tunnel-diode susceptance at band center and the latter provides a broad-band low-impedance RF ground. The tuned and stabilized tunnel diode, having the thin-film microstrip geometry and the RF equivalent circuit included in Figs. 2 and 4(a), respectively, was fabricated on a 1-in^2 alumina substrate and tested as a single-tuned TDA in conjunction with a commercially available circulator. The measured single-peaked gain response of this breadboard amplifier, exhibiting a 9.5-dB maximum gain and centered at 9.85 GHz with an 830-MHz half-power bandwidth, not only demonstrated the suitability of the inductive tuning element design, but verified the assumed equivalent circuit parameters of the tunnel diodes under consideration[4]

[4] Aertech A1G-225D (Ge) or AIA-225D (GaAs) having nominally identical equivalent-circuit parameters (see Fig. 4(a)).

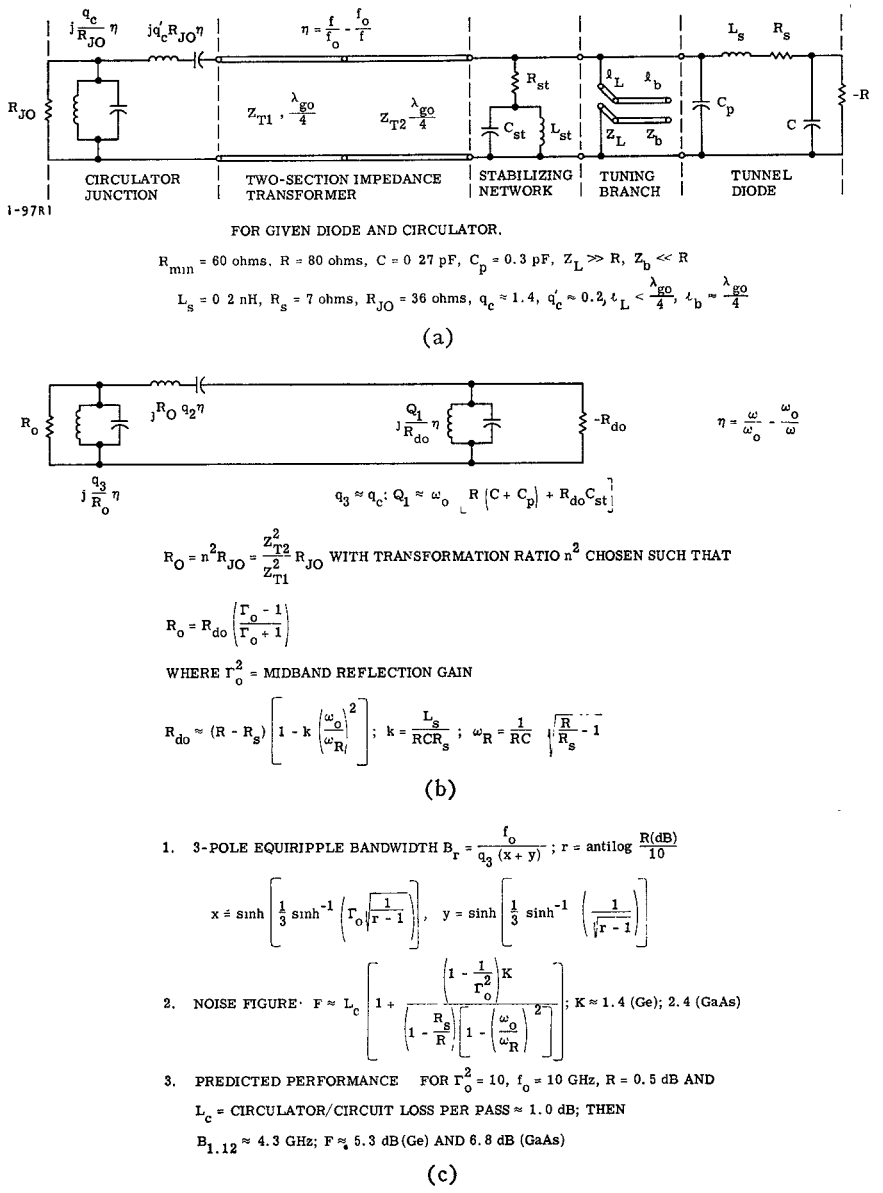

Fig. 4. Equivalent circuit representation of single-stage TDA. (a) Lumped equivalent circuit. (b) Passband prototype equivalent circuit. (c) Predicted performance parameters.

(see Fig. 4(a)). Completion of the individual design, and characterization of the circulator and the tuned and stabilized tunnel diode constituted the first major steps in the development of the thin-film microstrip TDA stages.

B. Development of Single-Stage MIC TDA

The measured data obtained during the development of the individual components, comprising the single-stage thin-film microstrip TDA under consideration (Fig. 2), permitted the implementation of a three-pole broad-banding design for the TDA stage [10] using the RF equivalent circuits shown in Fig. 4(a) and (b). In particular, the circuit representation of the TDA at the amplifier port of the circulator (Fig. 4(a)) includes a two-section transmission-line impedance transformer between the circulator junction and the tuned and stabilized tunnel diode. Optimum design of this transformer simultaneously provides the necessary impedance-level transformation from circulator junction-to-diode to establish the desired midband gain level, and provides the required frequency dependence necessary to synthesize the specified three-pole gain response.

This is suggested by the passband equivalent circuit of Fig. 4(b) in which a three-pole bandpass ladder network, interposed between the transformed circulator impedance level R_0 and the tunnel diode net negative resistance $-R_{d0}$, is synthesized to yield a three-pole equiripple reflection gain response. Consideration of the constraints on the end resonators, introduced by the circulator (q_c) and the tuned and stabilized tunnel diode, indicates [10] that the primary bandwidth restriction on this TDA design is imposed by the circulator.

Accordingly, the first-order gain-bandwidth and noise performance calculations on this configuration [1], [10], presented in Fig. 4(c), indicate the feasibility of achiev-

TABLE I

Tunnel diode	AIG-225D	AIA-225D	AIG-225D	AIA-225D
Semiconductor	Ge	GaAs	Ge	GaAs
Passband (GHz)	7.8 to 11.5	8.0 to 11.5	8.0 to 11.6	8.0 to 11.4
Passband gain (dB)	8.4 ± 1.0	10.0 ± 2.0	9.0 ± 1.0	10.0 ± 1.0
Passband noise figure (dB)	5.75 ± 0.4	7.2 ± 0.6	5.5 ± 0.5	8.0 ± 0.6
Output level at 1-dB gain compression (dBm)	−23 to −20	−17 to −14	−23.5 to −20	−19 to −13

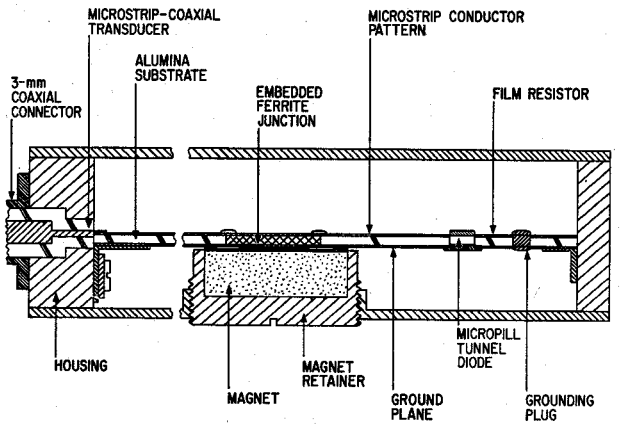

Fig. 5. Single-stage microstrip TDA, cross section.

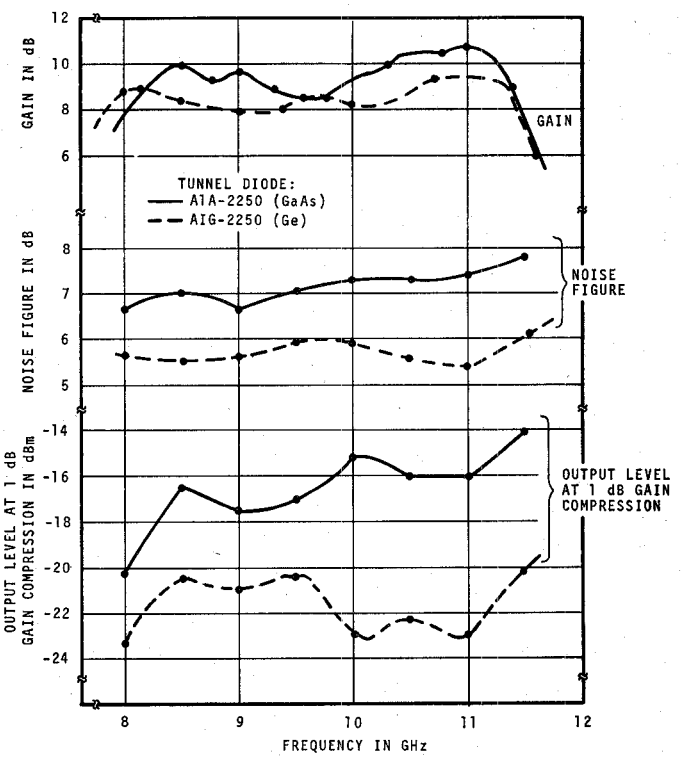

Fig. 6. Measured performance of single-stage 8- to 12-GHz TDAs.

ing an 8-dB three-pole 0.5-dB equiripple overall gain response with noise figure in the 5- to 7-dB range. A more refined synthesis of the amplifier–port matching network was conducted using computer-aided iterative techniques to optimize the lengths and impedances of the two-section transformer and parallel tuning branches, starting from their first-order values and then using more exact representations of the circulator junction and stabilized tunnel-diode impedance loci. The optimum predicted gain response obtained in this fashion, exhibiting a 6.2 ± 1.2-dB overall gain over 8 to 12 GHz, was somewhat degraded from that based upon the more idealized first-order representation.

Based upon this design, a series of single-stage 8- to 12-GHz thin-film microstrip TDAs were fabricated in the configuration of Fig. 2, using Ge and GaAs tunnel diodes of nominally identical equivalent circuit elements. A cross section of this TDA structure (Fig. 5) shows the details of the shunt-mounting geometry for the encapsulated tunnel diode, the circulator junction and magnet mounting, the incorporation of the substrate in the housing, and the compensated coaxial-to-microstrip transducer. The latter typically exhibits a ratio of less than 1.15:1 VSWR over the 8- to 12-GHz frequency range [2].

The measured performance of these amplifiers, using each evaluated in its own test housing, is summarized in Table I.

The gain, noise figure, and output level at 1-dB gain compression for representative TDAs using a Ge and GaAs tunnel diode are shown graphically as functions of frequency in Fig. 6.

This measured single-stage TDA performance is essentially as predicted ([1] and Fig. 4(c)), with the tradeoff between noise performance and large-signal linearity, represented by the choice of a Ge and GaAs tunnel diode, quite apparent. Accordingly, these single TDA stages were used as the building blocks for the dual-stage TDAs to be subsequently described.

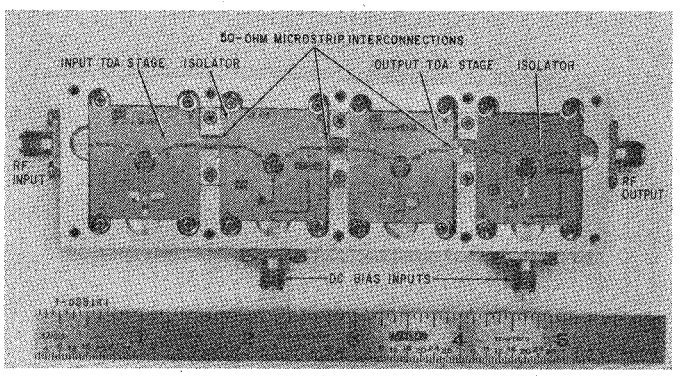

Fig. 7. Two-stage 8- to 12-GHz thin-film microstrip TDA.

C. A Dual-Stage MIC TDA

A two-stage thin-film microstrip 8- to 12-GHz TDA, shown in Fig. 7, consists of one each of the previously described Ge and GaAs TDA stages incorporated with their own associated output isolator in a partitioned aluminum housing. The Ge TDA and the GaAs TDA

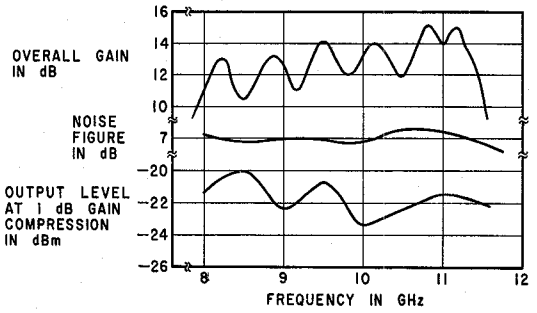

Fig. 8. Measured performance of two-stage 8- to 12-GHz TDA.

are deployed as the input and output stages, respectively, to simultaneously optimize noise figure and dynamic range [1], [7]. The 1-in² substrates comprising each TDA stage and isolator are each enclosed in a separate compartment. The intersubstrate connections are formed via short sections of 50-Ω line embedded in the partition walls. This level of integration, though not as complete as incorporating the two TDA stages and the two isolators on a single substrate, has the advantages of permitting pretesting of individual components, preventing spurious radiative coupling between components, and minimizing higher order "surface wave" mode propagation and "box resonances" associated with each component. These features are particularly important upon incorporation of the TDA in a more extensive receiver subassembly. The effect of box resonances in TDAs is more pronounced than in most components since they can readily excite out-of-band oscillations which are not suppressed by the microstrip stabilizing network at any frequency below the tunnel-diode resistive cutoff frequency. Therefore, the use of compartmentalization in MIC TDA construction becomes more necessary than for most other MIC components.

An all-microstrip approach to achieving the interconnections between adjacent microstrip components used short sections of 50-Ω microstrip line on small alumina substrates embedded in the partition walls and electrically connected to the adjacent components by welded ribbon leads. These transitions were virtually reflectionless; their measured VSWR over the 8- to 12-GHz band was well below the 1.15:1 maximum due to the 3-mm input coaxial connector and its associated transition. The resulting two-stage TDA configuration (Fig. 7) exhibited a measured performance over the 8.0- to 11.5-GHz frequency range (see Fig. 8) as follows:

1) average passband gain: 11.5 to 13.5 dB, monotonically increasing over 8.0 to 11.5 GHz;
2) passband gain ripple: 3 dB peak-to-peak;
3) passband noise figure: 6.8 to 7.2 dB;
4) output level at 1-dB gain compression: −20 to −23 dBm.

With reference to this measured performance, further

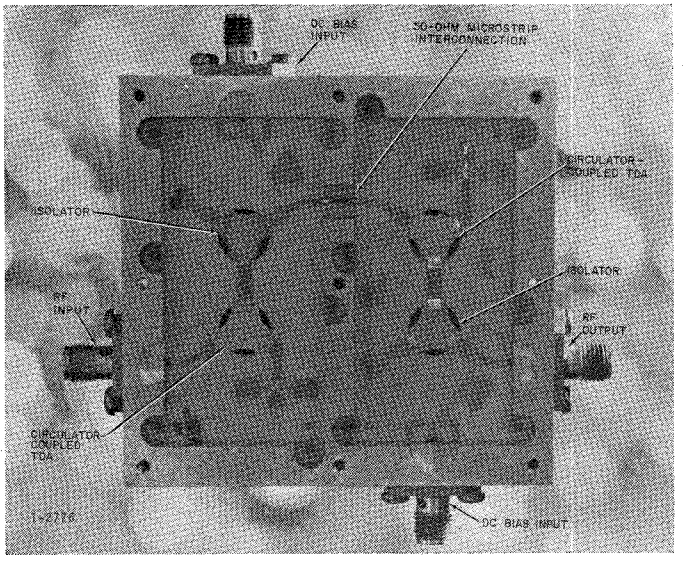

Fig. 9. Two-stage 6- to 8-GHz thin-film microstrip TDA.

improvement in amplifier passband gain flatness requires a) more careful apportioning of the gain tilt in each TDA stage to compenstate for that in the isolators, and b) improvement in the inherent circulator isolation to reduce the input–output mismatch interaction at each amplifier–isolator interface, and thereby much of the corresponding passband gain ripple. The degradation in input noise figure and output 1-dB gain-compression level, over that obtainable individually from a Ge tunnel-diode input stage and a GaAs tunnel-diode output stage, respectively, is due to output-stage contributions to the former and input-stage contributions to the latter.

Further improvement in the gain flatness of a two-stage TDA cascade may be physically implemented in a closer integration of each output isolator with its corresponding TDA stage by forming both on a single substrate with an optimized half-wavelength interjunction between the two ferrite elements. This level of integration is exemplified by the two-stage 6- to 8-GHz MIC TDA which is described in the following section.

IV. A 6- to 8-GHz MIC TDA

Fig. 9 shows a closely integrated two-stage thin-film microstrip 6- to 8-GHz TDA cascade. It consists of a partitioned aluminum housing containing a Ge TD input stage and a GaAs TD output stage, each of which is closely integrated with its associated output isolator on a 1- by 2-in alumina substrate. A 50-Ω microstrip bridge on a small substrate embedded in the housing partition wall forms the interconnection between the two individually enclosed substrates.

The individual elements and components comprising each amplifier/isolator stage use the same approach to electrical design, and hence are identical in geometry to those employed in the previously described 8- to 12-

GHz TDA but with the dimensions scaled to a center frequency of 7 GHz. The major innovation in the 6- to 8-GHz TDA realization is the close integration of each TDA stage and its associated output isolator on a single 1- by 2-in substrate, with an optimum-impedance half-wavelength transmission line interconnecting the two embedded ferrite junctions.[5]

The measured performance of the dual-circulator cascade, comprising the amplifier-coupling mechanism and output isolator associated with each stage, includes monotonic two-pass insertion loss and isolation responses of 0.5 to 1.5 dB and 40 to 43 dB, respectively, over the 5.6- to 7.6-GHz range. The relative flatness of the two-pass isolation and insertion-loss responses indicates a minimum of impedance interaction on the circulator–isolator interjunction arm (which was not necessarily the case in the cascaded 8- to 12-GHz configurations).

The improvement in gain flatness, achievable by using these closely integrated amplifier/isolator stages as building blocks in a two-stage cascade, is exemplified by the measured performance of two models of the thin-film microstrip TDA (Fig. 9). The measured characteristics of these two-stage TDAs (Fig. 10) may be summarized as follows.[6]

Model	I	II
Passband (GHz)	6.25 to 7.75	6.2 to 7.65
Passband gain (dB)	12.0 ± 1.0	12.6 ± 0.8
Passband noise figure (dB)	6.4 to 7.4	6.4 to 7.8
Passband output level at 1-dB gain compression (dBm)	−20 ± 4	−20.5 ± 3.5

These results indicate that the close integration of each amplifier/isolator stage makes possible a high degree of unit-to-unit reproducibility as well as providing improved flatness in a two-stage cascaded configuration.

V. Conclusions

The measured level of performance of the two-stage TDAs described herein (Figs. 8 and 10) is generally satisfactory for use in the type of high-performance receiver under consideration, particularly in combination with some external means for dynamic range extension [1]. Nonetheless, further improvement in the performance of MIC TDAs for this application should be achievable by concentration of effort in each of the following areas.

1) Through a further improvement in the isolation-bandwidth product of the MIC circulators for a corresponding improvement in the TDA gain-bandwidth product or gain-flatness within a given band.

2) An extension of cascading to a multistage TDA configuration, in which more than one Ge and GaAs tunnel-diode input and output stages are used, respectively (maintains low noise figure and maximum dynamic range). This leads to higher overall gain capability in a given bandwidth, and thereby provides a greater reduction in the noise contribution of components following the TDA in the receiver configuration under consideration.

3) The use of low-impedance and/or multiple GaAs tunnel diodes in the output stage for further enhancement of large signal linearity.

4) The use of unencapsulated tunnel diodes promote, by virtue of further reduction in parasitics, greater gain-bandwidth capability and greater ease in incorporation of low-impedance or multiple tunnel diodes, as previously described.

These TDAs, however, represent the starting point for achieving the next generation in MIC TDA performance.

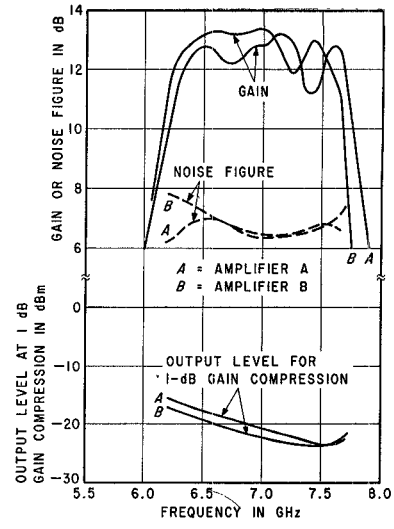

Fig. 10. Measured performance of two-stage 6- to 8-GHz TDA.

Acknowledgment

The authors wish to thank R. Runnels and D. Rees of the Air Force Avionics Laboratory, for their direction and encouragement, H. Gable for the design of the circuit housings, A. Kunze for the processing of the thin-film circuits, and R. Chew for assembling and testing the thin-film circuits. They also wish to thank S. Okwit, J. G. Smith, and J. Taub for their advice and encouragement.

References

[1] A. Leber and H. Okean, "Tunnel-diode amplifiers as components in wide dynamic range systems," *WESCON Tech. Papers*, vol. 12, pp. 5/2-1–5/2-9, Aug. 1968.
[2] P. J. Meier, H. C. Okean, and E. W. Sard, "Integrated *X*-band sweeping superhetereodyne receiver," *IEEE Trans. Microwave Theory Tech. (Special Issue on Microwave Integrated Circuits)*, vol. MTT-19, pp. 600–609, July 1971.
[3] N. E. Feldman, "Syllabus on low noise microwave devices," *Microwave J.*, vol. 12, pp. 59–69, July 1969.

[5] Xtalonics X-1200 (1200-G saturation magnetization) polycrystalline YIG disk.
[6] The input and output stages of these amplifiers use Aertech AIG-225D (Ge) and AIA-220D (GaAs) tunnel diodes, respectively.

[4] W. G. Matthei and W. Crowe, "New microwave integrated circuit modules," *WESCON Tech. Papers*, vol. 12, pp. 2/1-1–2/1-6, Aug. 1968.
[5] H. C. Okean, "Microwave amplifiers employing integrated tunnel-diode devices," *IEEE Trans. Microwave Theory Tech.*, vol. MTT-15, pp. 613–622, Nov. 1967.
[6] J. D. Welch, "Beam lead tunnel-diode amplifiers on microstrip," in *1970 G-MTT Int. Symp. Dig.*, pp. 212–216, 1970.
[7] R. Steinhoff and F. Sterzer, "Microwave tunnel-diode amplifiers with large dynamic range," *RCA Rev.*, vol. 25, pp. 54–66, Mar. 1964.
[8] S. Virk, "The state of tunnel-diode technology," *Electron. Products*, pp. 30–32, Nov. 1969.
[9] A. Lueck, W. Schultz, and A. Marmiani, "The solid structure tunnel diode," *Microwave J.*, vol. 9, pp. 49–52, July 1966.
[10] H. C. Okean, "Synthesis of negative resistance reflection amplifiers employing band-limited circulator," *IEEE Trans. Microwave Theory Tech.*, vol. MTT-14, pp. 323–337, July 1966.

Correspondence

Slot-Line Field Components

SEYMOUR B. COHN

***Abstract*—Formulas derived by mode summation give the six E- and H-field components in the various air and dielectric regions of a slot-line cross section. These formulas are valid except when very close to the slot, where approximations in the analysis cause a large error. A quasi-static method yields a second set of formulas that apply near the slot. Thus the field is determined satisfactorily in all parts of the cross section. Graphs of the H components show that elliptical polarization exists, with the best approach to circularity near the slot and near the opposite surface of the substrate. Quantitative field data are useful for analysis and design of slot-line components, such as ferrite devices, dielectric-resonator filters, directional couplers, and broad-band transitions to coaxial line or microstrip.**

I. Introduction

Several earlier papers [1]–[7] show that slot line has interesting potentialities for microwave integrated circuits on dielectric substrates. The analysis of slot-line wavelength, group velocity, and characteristic impedance [1] has been extended to yield the field components as functions of frequency, slot-line constants, and coordinates in the air and substrate regions.

Elliptic polarization of the magnetic field makes quantitative field data especially pertinent for ferrite components and YIG resonators. Knowledge of the field is also useful in the design of slot-excited dielectric resonators and directional couplers between two slots or a slot and microstrip. Application of the field formulas is also used in deriving equivalent circuits for transitions between slot line and coaxial line.

The formulas in this correspondence apply also to *sandwich* slot line; that is, a slotted metal sheet sandwiched between two substrates [5], [8].

Manuscript received February 26, 1971; revised June 28, 1971. This work was performed for Stanford Research Institute as a part of their study program for the U. S. Army Electronics Command under Contracts DAAB07-68-C-0088 and DAAB07-70-C-0044.
The author is a consultant to Stanford Research Institute, Menlo Park, Calif.

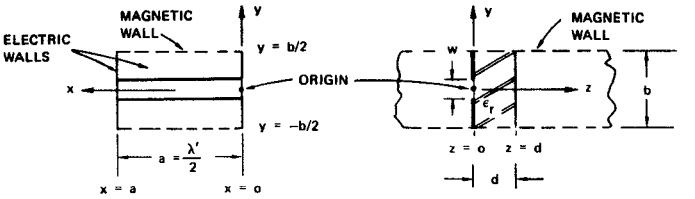

Fig. 1. Waveguide model used in field-distribution analysis.

II. Field Components

The configuration considered here is shown in Fig. 1. As in the earlier analysis [1], the slot-line problem is reduced to a rectangular waveguide problem by inserting electric walls in the planes perpendicular to the slot at $x=0$ and $x=a=\lambda'/2$, and magnetic walls at $y=\pm b/2$.

A pair of slot-line waves travel in the $+x$ and $-x$ direction with wavelength λ' substantially smaller than the free-space wavelength λ. For b sufficiently large (typically $b>\lambda'$), the fields at the magnetic walls are very small, and therefore b has negligible effect on the fields near the slot.

On the air side of the slot ($z\leq 0$), five field components exist: E_y, E_z, H_x, H_y, and H_z. On the substrate side these plus E_x exist. The coordinates x, y, z, the dimensions w, d, b, and the relative permittivity ϵ_r are all defined in Fig. 1. A factor $e^{j(\omega t-2\pi x/\lambda')}$ is assumed for each field component implying wave propagation in the $+x$ direction only. V_0 is the voltage directly across the slot.

The complete set of field-component formulas is contained in a